journal

J. Am. Ceram. Soc., 76 [1] 139–44 (1993)

# Effect of Loading Mode and Coating on Dynamic Fatigue of Optical Fiber in Two-Point Bending

Vincenzo V. Rondinella* and M. John Matthewson*

Fiber Optic Materials Research Program, Department of Ceramic Science and Engineering, Rutgers University, Piscataway, New Jersey 08855–0909

**Two-point bending is a useful method for investigating the mechanical properties of optical fiber and has several advantages when compared to the traditional tensile test. However, the strength of the fiber is usually determined at constant faceplate velocity rather than at constant strain rate as in the uniaxial tensile test, and previous work casts doubt on the comparability of fatigue results obtained using different loading modes and hence on the reliability of the bending technique. This paper presents dynamic fatigue results using a two-point bend apparatus that can be programmed to operate in constant velocity, constant strain rate, and constant stress rate loading modes. These results, obtained for both bare and polymer-coated fused silica optical fiber, show no significant differences in the calculated fatigue parameters for the three loading modes and clearly indicate the reliability of the two-point bend method at constant faceplate velocity. The results, however, show that the obtained value of the stress corrosion susceptibility parameter, *n*, is dependent on the quantity used to define it, i.e., stress or strain to failure, because of the nonlinear elastic behavior of silica.**

## I. Introduction

FUSED silica optical fiber is used for a variety of applications, some of which, such as long-haul telecommunications, involve very long lengths of fiber that might be exposed to adverse environments. The mechanical reliability of such fiber systems is a matter of concern, since silica glass is subject to delayed failure, or fatigue, under the combined influence of stress and environmental moisture. Therefore, to assess reliability it is necessary to determine the mechanical properties of the fiber in terms of strength and fatigue behavior.

The most important methods for determining the mechanical properties of high-strength fiber are loading in tension and two-point bending. While the two methods have been compared in detail elsewhere,[1] the methods contrast each other in two key areas: tested length and experimental convenience.

In comparison to the tensile test, the two-point bend method (Fig. 1) does not present gripping problems, since the specimen is nominally subjected to zero bending stress where it contacts the two faceplates. Furthermore, it is a very simple technique to perform, as it allows the fiber to be easily immersed in a test environment. A possible disadvantage of two-point bending is that the tested length of fiber is only a few tens of micrometers[1] so that the results are of limited use in evaluating long-length behavior.

The strengths of the fiber measured in bending and tension differ numerically for two reasons. First, the very different test length of the two methods affects strength due to statistical variability (longer lengths are more likely to contain a more severe flaw and are therefore weaker), and this effect has been fully analyzed elsewhere.[1] Second, the strength is well-known to depend on loading rate, since lower rates give more time for environmental moisture to degrade the fiber strength. Therefore, strengths in bending and tension should be measured under equivalent fatigue conditions for a fair comparison to be made. In its simplest and most common application the faceplates of a two-point bend apparatus are brought together at constant velocity. Because of the nonlinear relationship between the stress on the fiber and the faceplate gap, the loading rate increases as the experiment progresses (see Eq. (1)). In contrast, tensile experiments are almost always conducted at a constant displacement rate which approximates a constant stressing rate, so that under these circumstances bending and tension are not directly comparable. The difference in loading mode can be accounted for when calculating fatigue parameters if the power law subcritical crack growth model for fatigue is used.

Yuce *et al.*[2] used a two-point bend system in which the velocity of the faceplates could be varied during the experiment. In

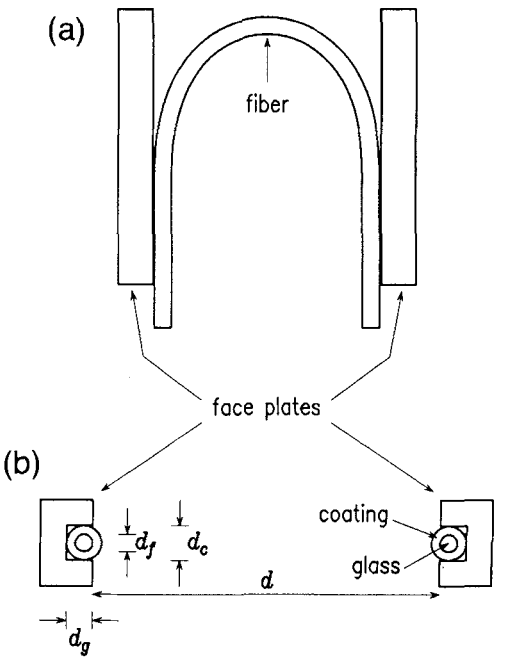


**Fig. 1.** Schematic of the two-point bend apparatus in (a) plan and (b) section. Note that the denominator in Eq. (1) is the distance between the neutral axes of the two arms of the fiber.

T. A. Michalske—contributing editor

Manuscript No. 195899. Received March 13, 1992; approved September 10, 1992.

*Member, American Ceramic Society.

this way they were able to directly compare the fatigue parameter, $n$, for silica fiber determined in bending under conditions of constant faceplate velocity, constant stress rate, and constant strain rate (the latter two are not equivalent because of the strain dependence of the elastic modulus of silica). Their results showed significant differences in the value of $n$ found for the three different loading modes. This observation has three important implications. First, it would appear to invalidate two-point bending measurements made at constant faceplate velocity for determining fatigue parameters to be applied to constant stress rate conditions. Second, since the differences are not predicted by the subcritical crack growth model for fatigue, the results of Yuce *et al.*[2] cast doubt on the applicability of this model. In fact, this model may be criticized on physical grounds because high-strength silica fiber does not contain sharp, well-defined cracks,[3] but additionally, Yuce's work would indicate that the model is not useful even as an empirical scaling law. Third, differences in results for the different loading modes could be used to determine a new empirical model for fatigue.

The purpose of this paper is to investigate the different loading modes in two-point bending to determine whether they do give consistently different results. In fact, we find they do not give different results, and there is therefore no inconsistency with the subcritical crack growth model. Hence, this model is at least applicable as a scaling rule for these short-duration dynamic fatigue experiments.

The stress corrosion susceptibility parameter, $n$, is normally defined from fatigue data that quantify the strength by the failure stress, $\sigma_f$. However, bending tests measure failure strain, $\varepsilon_f$, directly, and failure stress indirectly via the elastic modulus. It would therefore be convenient to use failure strain to determine $n$, since no knowledge of the elastic modulus is then required. However, while $n$ for high-strength silica is found to be independent of the loading mode, it is found to depend on whether $\sigma_f$ or $\varepsilon_f$ is used to define it. This observation results from the nonlinear elastic behavior of silica observed at high strain (>1%) and so is relevant only to the high-strength material.

## II. Theory

The maximum strain on the fiber when it fails, $\varepsilon_f$, occurs at the tip of the bend and is calculated from the gap between the faceplates at failure, $d$, using[4]

$$\varepsilon_f = 1.198 \frac{d_f}{(d - d_c + 2d_g)} \tag{1}$$

where $d_f$ is the glass fiber diameter, $d_c$ is the overall fiber diameter including any coating, and $2d_g$ is the total depth of both grooves (see Fig. 1).

The empirical relationship between the rate of growth of a macroscopic crack, $\dot{c}$, and the applied stress intensity factor, $K_I$, is given by[5]

$$\dot{c} = AK_I^n \tag{2}$$

where $n$ is the stress corrosion susceptibility parameter and $A$ is a constant depending on the environment. When combined with the well-known Griffith equation,

$$K_I = \sigma Y c^{1/2} \tag{3}$$

where $Y$ is a constant depending on the geometry of the crack, these equations may be integrated, once the loading mode is specified, to obtain the fatigue equation relating the strength and the loading rate.

### *(1) n from Failure Stress*

Wiederhorn[5] shows that under conditions of constant stress rate ($\dot{\sigma}$ constant) the strength is related to the loading rate by

$$\sigma_f^{n+1} = \frac{(n+1)}{(n-2)} \frac{2}{AY^2} \left(\frac{\sigma_{IC}}{K_{IC}}\right)^{n-2} \dot{\sigma} = B\dot{\sigma} \tag{4}$$

where

$$B = \frac{(n+1)}{(n-2)} \frac{2}{AY^2} \left(\frac{\sigma_{IC}}{K_{IC}}\right)^{n-2} \tag{5}$$

$\sigma_{IC}$ is the inert or intrinsic strength of the fiber in the absence of fatigue and $K_{IC}$ is the critical stress intensity factor. Equation (4) can be reformulated for a constant strain rate by substituting $E\dot{\varepsilon} = \dot{\sigma}$, where $E$ is Young's modulus.

France *et al.*[6] show that, under conditions of constant faceplate velocity ($v = \dot{d}$), Eq. (1), when combined with (2) and (3), relates the failure stress to the faceplate velocity, $v$, by

$$\sigma_f^{n-1} = \frac{(n-1)}{(n-2)} \frac{0.835}{rEAY^2} \left(\frac{\sigma_{IC}}{K_{IC}}\right)^{n-2} v \tag{6}$$

where $r$ is the radius of the fiber ($2r = d_f$).

It is well-known that Eqs. (4) and (6) are linearized on a double logarithmic plot of strength versus loading rate[5,6] and that the fatigue parameters are calculated from the slope and intercept. The slopes and intercepts for the three loading modes are summarized in Table I. According to the subcritical crack growth model, there is no reason why the values of $n$ determined for the three loading modes ($n_\sigma$, $n_\varepsilon$, $n_v$ for constant stress rate, strain rate, and velocity, respectively) should be different.

### *(2) n from Failure Strain*

In the above analyses, the strength has been characterized by the failure stress. However, as mentioned above, bending directly measures the strain, and so it is convenient to characterize the strength by the failure strain. These two approaches are equivalent if Young's modulus of the material, $E$, is a constant. However, the modulus of fused silica is sensitive to the strain for strains in excess of 1%. Therefore, the value of $n$ will be different if it is determined from the slope of a log $\varepsilon_f$ versus log (rate) plot rather than a log $\sigma_f$ versus log (rate) plot. We will now investigate the magnitude of this effect.

The strain dependence of the elastic modulus is given empirically by

$$E(\varepsilon) = E_0(1 + \alpha\varepsilon + \beta\varepsilon^2) \tag{7}$$

where $E(\varepsilon)$ is Young's modulus at a strain $\varepsilon$, and $E_0$ is the modulus at zero strain. Values of $E_0 = 72.2$ GPa, $\alpha = 3.2$, and $\beta = 8.48$ are used, which are calculated from the acoustic measurements up to 6% strain of Krause *et al.*[7]

Considering an experiment conducted under conditions of constant rate, $\rho$ (where $\rho$ can be replaced by $\dot{\sigma}$, $\dot{\varepsilon}$, or $v$), the slope derived from a log $\varepsilon_f$ versus log $\rho$ plot is given by

$$m_\rho^\varepsilon = \frac{d \log \varepsilon_f}{d \log \rho} \tag{8}$$

while that derived from a log $\sigma_f$ versus log $\dot{\sigma}$ plot is given by

$$m_\rho^\sigma = \frac{d \log \sigma_f}{d \log \rho} \tag{9}$$

where the superscript defines whether failure strain or stress is used. It can readily be shown that

**Table I. Slopes and Intercepts of log $s_f$ versus log (Loading Rate) Fatigue Plots for the Three Loading Modes**

| | Slope, $m$ | Intercept, $c$ |
|---|---|---|
| Constant $v$ | $\frac{1}{n-1}$ | $\frac{1}{n-1} \log \left(\frac{0.417B(n-1)}{Er(n+1)}\right)$ |
| Constant $\dot{\varepsilon}$ | $\frac{1}{n+1}$ | $\frac{1}{n+1} \log (BE)$ |
| Constant $\dot{\sigma}$ | $\frac{1}{n+1}$ | $\frac{1}{n+1} \log B$ |

$$m_\rho^\sigma = m_\rho^\varepsilon \frac{d \log \sigma_f}{d \log \varepsilon_f} = m_\rho^\varepsilon \left(1 + \frac{d \log E}{d \log \varepsilon_f}\right) \tag{10}$$

Using the appropriate relations in Table I between $m$ and $n$, the $n$ values determined from failure strain and failure stress are related by

$$n_\rho^\varepsilon = n_\rho^\sigma (1 + \zeta) + \zeta \qquad \text{when } \rho = \dot{\sigma} \text{ or } \dot{\varepsilon} \tag{11}$$

or

$$n_\rho^\varepsilon = n_\rho^\sigma (1 + \zeta) - \zeta \qquad \text{when } \rho = v \tag{12}$$

where

$$\zeta = \frac{(\alpha\varepsilon_f + 2\beta\varepsilon_f^2)}{(1 + \alpha\varepsilon_f + \beta\varepsilon_f^2)} = \frac{d \log E}{d \log \varepsilon_f} \tag{13}$$

Ignoring terms $O[\varepsilon_f^3]$,

$$\zeta \approx \alpha\varepsilon_f + (2\beta - \alpha^2)\varepsilon_f^2 \tag{14}$$

By substituting values of $\varepsilon_f = 5\%$ and $n^\sigma = 20$, typical for a high-strength fiber, Eq. (11) predicts a value of $n^\varepsilon = 23.6$. This represents a significant error, and therefore, to be consistent, $n$ should be determined from failure stress, or at least the method for determining it should be clearly specified. Throughout this work, $n$ has been determined using failure stress and elastic modulus parameters $E_0 = 72.2$ GPa, $\alpha = 3.2$, and $\beta = 8.48$.[7] The values of $n^\varepsilon$ have also been determined, and the differences between the values of $n^\varepsilon$ and $n^\sigma$ obtained from the experimental data agree with the differences calculated using Eq. (11).

It is noted that the term in $\varepsilon_f^2$ in Eq. (14) is small compared to the term in $\varepsilon_f$ so that the second-order modulus correction is insignificant for this calculation. Therefore, similar results are obtained if a simpler form of the modulus strain dependence given by Glaesemann *et al.*[8] is used, for which $\alpha = 3$ and $\beta = 0$.

## III. Experimental Procedure

Dynamic fatigue experiments were performed using the two-point bend apparatus shown schematically in Fig. 1. The fiber is bent between two faceplates that are brought together by a computer-controlled stepper motor until the fiber breaks. An acoustic transducer and trigger circuit detects the break and halts the stepper motor. For coated fiber, grooved faceplates are used to locate the fiber accurately.[4] The sharp groove edges, however, would damage bare fiber, causing premature failure. Therefore, bare fiber is balanced between polished faceplates and loosely held in position by lightly clamping to a plate perpendicular to the faceplates, as shown in Fig. 2.[1]

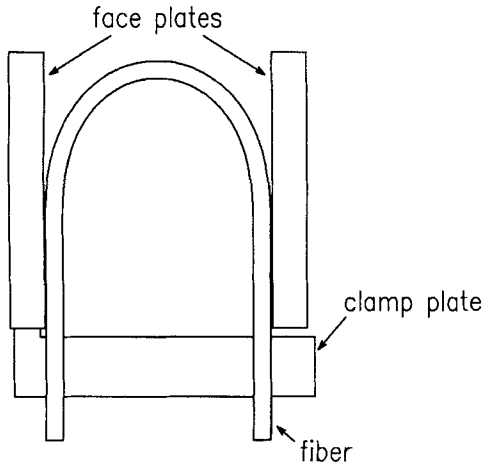


**Fig. 2.** Schematic of the two-point bend apparatus used for breaking bare fiber.

For the constant stress and strain rate experiments, the stepping rate of the motor used to drive the faceplates was continuously varied during the test.[2,9] Differentiation of Eq. (1) with respect to time gives

$$\dot{\varepsilon} = \frac{1.198 d_f}{(d - d_c + 2d_g)^2} \dot{d} \tag{15}$$

so that, for example, in a constant strain rate experiment, the interval, $\Delta t$, between steps of length $\delta$, ($\delta = \dot{d}\Delta t$) is given by

$$\Delta t = \frac{1.198 d_f}{(d - d_c + 2d_g)^2} \frac{\delta}{\dot{\varepsilon}} \tag{16}$$

This equation is used to calculate the time interval between each individual step, with care taken to avoid propagation of rounding and truncation errors; by using 1 μm per step and a 1-kHz timing clock, the error in the faceplate position is always less than 0.5 μm and 0.5 ms. This ensures that the loading profile is not a source of error. Approximating the velocity profile by several constant-velocity segments would also be satisfactory, provided the segments are sufficiently short.

Table II summarizes the rates used for the different loading modes. The total interval spans three decades; these rates are the same as those used by Yuce *et al.*,[2] who chose them to give the same faceplate velocity at the beginning of each corresponding experiment, when the plate separation is 13 mm.

The fiber used in this study was a 125-μm-diameter fused silica coated with a UV-curable polyurethane-acrylate. The overall measured diameter of the coated fiber was 242 μm. The polymer coating confuses fatigue results since it acts, at the least, as a diffusion barrier to the environment and introduces additional time effects. For this reason, bare fiber was also studied in order to directly evaluate the fatigue behavior of the silica. The bare fiber was obtained by stripping the coating from a length of fiber by briefly dipping in hot (200°C) concentrated sulfuric acid followed by rinsing in acetone and then water.

The strength measurements were, unless otherwise indicated, performed in a standardized environment of pH 7 phosphate buffer solution. This environment was chosen, rather than deionized water or air, in order to maintain a chemically stable and reproducible environment. The pH of water can change with time if exposed to air, which would influence the results due to the pH dependence of strength (e.g., Refs. 10 and 11). The use of the pH 7 environment is more convenient than attempting to control the humidity of an air environment.

The environmental barrier offered by the coating for the short-duration tests (corresponding to the highest loading rates, with a time scale of ~10 s) is less effective when the duration of the experiment is relatively large (i.e., at the lowest loading rates whose time scale is $\sim 10^5$ s). This means that for coated fiber the effect of the environment may systematically change with loading rate. In order to eliminate this effect, bare fiber has also been studied. With bare fiber, the surface of the glass is directly and immediately in contact with the test solution. Since fatigue studies are concerned with the effects of environmental agents on the silica, uncoated fiber directly examines these interactions.

Unless otherwise stated, all coated fibers were presoaked before testing for 24 h at room temperature in pH 7 solution in order to minimize environmental equilibration effects.

**Table II. Loading Rates Used in the Three Types of Loading Mode Experiment**

| Constant $v$ (μm·s$^{-1}$) | Constant $\dot{\varepsilon}$ (%·min$^{-1}$) | Constant $\dot{\sigma}$ (MPa·s$^{-1}$) |
|---|---|---|
| 837 | 5 | 60 |
| 83.7 | 0.5 | 6 |
| 8.37 | 0.05 | 0.6 |
| 0.837 | 0.005 | 0.06 |

All the tests were performed at ambient laboratory temperature. The temperature of the test solution was measured for each specimen and typically fluctuated about the mean temperature of 22°C by ±2°C. The results were corrected to a reference temperature of 22°C (295 K), using the equation

$$\varepsilon_f(295) = \varepsilon_f(T)[1 + \lambda(T - 295)] \quad (17)$$

where $T$ is the test temperature in K, and $\lambda = 0.0149\ K^{-1}$. This relationship holds for a small temperature span,[12] and the value of $\lambda$ was determined in pH 7 buffer solution. The temperature correction is generally small and has little effect on the mean strength but can significantly reduce the scatter in results.

## IV. Results and Discussion

Figures 3 and 4 present the dynamic fatigue results for, respectively, bare and coated fiber. The failure stresses as a function of the rate of loading for the three modes, constant velocity, constant stress rate, and constant strain rate, closely fit straight lines on the log–log plots. Table III compares the slopes of the lines, $m$, together with the fatigue parameters, $n$ and log $B$, calculated from the slopes and intercepts. 95% confidence intervals for these values, found by doubling the standard errors, are also given. Log $B$ was calculated using a consistent set of units; stress in pascals, length in meters, time in seconds, and dimensionless strain.

The confidence intervals on $n$ are calculated from those on $m$. The confidence intervals on log $B$ are more complicated to determine since log $B$ depends on both the slope and intercept of the best fit line and these quantities are correlated. However, a detailed analysis accounting for the covariance has shown that the uncertainty in log $B$ is dominated by the uncertainty in the slope, so that

$$\Delta \log B \approx \frac{\Delta m}{m} \log B \quad (18)$$

A symmetrical confidence interval in $m$ leads to an asymmetrical confidence interval in $n$ and log $B$. However, the asymmetry is insignificant compared to the error in the errors and disappears on rounding to the values in Table III.

The values of $n$ in Table III are shown graphically in Fig. 5, together with the values of $n$ determined by Yuce *et al.*[2] Examination of Table III and Fig. 5 shows that for the data obtained in this work there is no significant difference between the values of $n$ and $B$ under different loading conditions, although the values are somewhat different for bare and coated fiber. Since $n$ and $B$ are independent of the loading mode, Eq. (6) shows that the same must be true for the fatigue preexponent, $A$, defined by Eq. (2). Therefore the measured values of both fatigue parameters, $n$ and $A$, are independent of loading mode for these experiments.

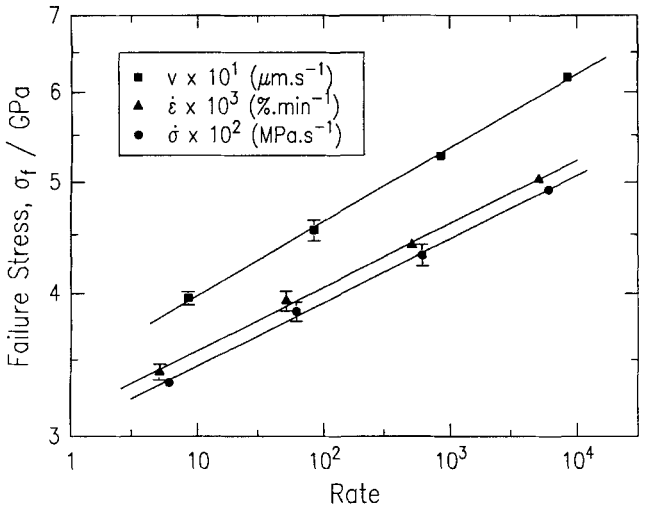


**Fig. 3.** Dynamic fatigue results for bare fiber. The failure stress is shown for constant velocity, constant strain rate, and constant stress rate loading modes.

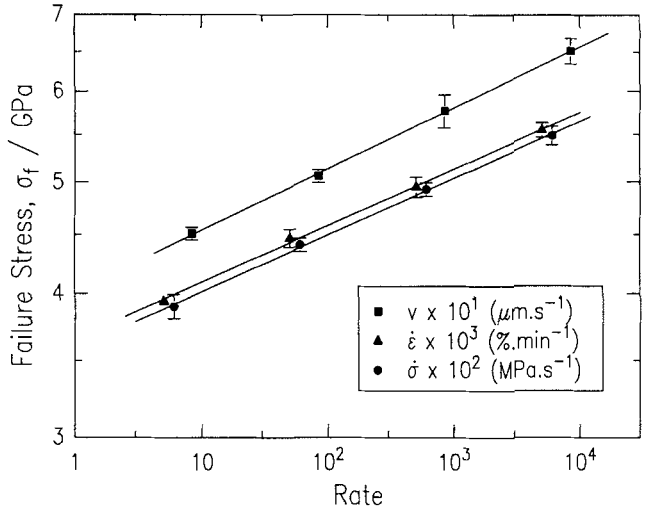


**Fig. 4.** Dynamic fatigue results for coated fiber at constant velocity, constant strain rate, and constant stress rate loading modes. The fibers were preconditioned in the test environment for 24 h before breaking.

The results of Table III show that, while the values of $n$ measured in the different loading modes are not significantly different, the fatigue plot slopes, $m$, measured at constant faceplate velocity are significantly different from the corresponding slopes measured at constant stress or strain rate. Therefore, the difference in form of the relationships between $m$ and $n$ in Table I is readily detectable within experiment error.

The invariance of $n$ and log $B$ with loading mode for bare fiber is a property of the silica (at least in these environments and loading rates). The results for coated fiber indicate that the invariance holds, at least for some coating systems. However, the results of Yuce *et al.*[2] show that fatigue can depend on the loading mode, and therefore this effect must be due to the coating.

### *(1) Alternative Crack Growth Kinetics Models*

The above analysis uses the empirical power law crack growth kinetics model (Eq. (2)) which has little physical significance. Several alternative models have been proposed, some of which are based on chemical kinetics models.[13,14] Trantina[13] showed that the static fatigue slopes for the different models are related. For example, when the simple exponential form of the crack growth kinetics,

$$\dot{c} = A' \exp(n' K_I) \quad (19)$$

and the power law model are fitted to the same data, the $n$ values are related by

$$n' \approx (n - 1)\frac{\sigma_{IC}}{\sigma_0} \quad (20)$$

where $\sigma_0$ is the "central" or average applied stress of the data. Similar relationships hold for other forms of the kinetics model for both the fatigue slopes and preexponents.[15] Matthewson[16] showed that the same relationships approximately hold for fitting to dynamic fatigue data. This indicates that, for a given set of data, there is a unique relationship between the fatigue parameters for the different kinetics models. Therefore, if the power law $n$ values are independent of the loading mode, the exponential $n'$ values are also independent of the loading mode, as are the slope parameters for all other models. Even though the analysis in this paper is cast in terms of the power law model, the conclusions are independent of the particular model

**Table III. Results for the Fatigue Parameters Measured under Different Loading Modes for Bare and Coated Fiber***

| | Constant $v$ | Constant $\dot{\varepsilon}$ | Constant $\dot{\sigma}$ |
|---|---|---|---|
| | | Bare | |
| $m$ | 0.0650 ± 0.0028 | 0.0555 ± 0.0027 | 0.0558 ± 0.0023 |
| $n$ | 16.4 ± 0.7 | 17.0 ± 0.9 | 16.9 ± 0.7 |
| $\log B$ | 161 ± 7 | 167 ± 8 | 166 ± 7 |
| | | Coated | |
| $m$ | 0.0529 ± 0.0023 | 0.0496 ± 0.0023 | 0.0490 ± 0.0026 |
| $n$ | 19.9 ± 0.8 | 19.2 ± 0.9 | 19.4 ± 1.1 |
| $\log B$ | 196 ± 8 | 189 ± 9 | 191 ± 10 |

*Errors represent a 95% confidence interval.

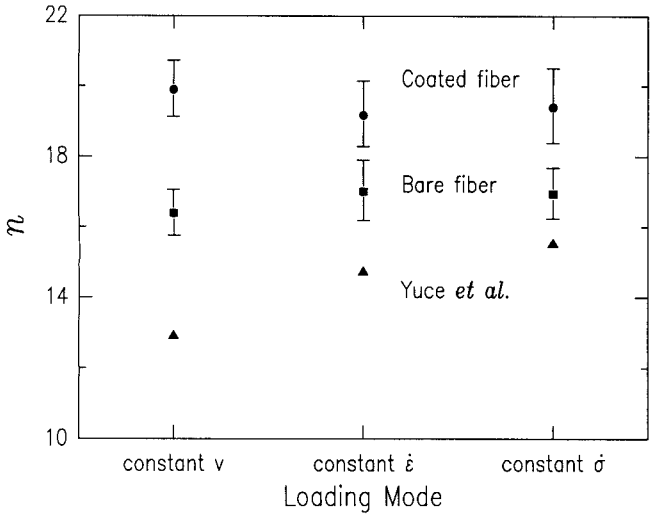


**Fig. 5.** Values of the stress corrosion susceptibility parameter, $n$, obtained from the three different loading modes for both coated and bare fiber. Values from Yuce *et al.*[2] are also shown for comparison.

used. It should be noted that, under dynamic fatigue conditions, the crack growth equations can be integrated analytically only for the power law, but must be integrated numerically for the exponential forms.[13,14,16]

### (2) *Effect of Preconditioning Time*

The results for coated fiber shown in Fig. 4 were obtained after the fiber had been preconditioned in the pH 7 buffer test environment for 24 h. This is necessary because the fibers are stored in ambient air and the diffusion time of liquid through the coating is comparable to the experimental duration of fatigue tests. Since the fiber is stronger in air than water, insufficient preconditioning time would decrease the apparent value of $n$, since the fastest loading rates, with failure times of the order of seconds, do not allow any further conditioning, while the slowest loading rates, with failure times of around 15 h, give lower strengths due to fatigue, but also due to the fiber being able to reach equilibrium with the more aggressive liquid environment. This effect is illustrated in Fig. 6, which compares the constant stress rate results of Fig. 4 with results of measurements made on the fiber with zero preconditioning time. At the highest loading rate of 60 MPa·s$^{-1}$, there is a significant difference between the preconditioned and nonpreconditioned fiber; the latter has a strength of 6.89 ± 0.04 GPa, which is the same as that of coated fiber tested in ambient air, namely 6.94 ± 0.02 GPa in 28% relative humidity (ambient air is the environment in which the fiber is stored). Therefore, testing at the highest rates without preconditioning is effectively testing in the storage environment. In contrast, there is little difference in strength between preconditioned and nonpreconditioned fiber tested at 0.06 MPa·s$^{-1}$, when the failure time is ~15 h. The nonpreconditioned fiber data show curvature, and linear regression gives a value of $n$ of 12 ± 5, which is considerably lower than the preconditioned value of 19.4 ± 1.1.

Figure 7 shows the effect of the preconditioning time on the fiber strength measured at a constant faceplate velocity of 1000 μm·s$^{-1}$, which gives a failure time of a few seconds. A systematic decrease in strength is observed with time, and there is no clear evidence that equilibrium has been reached after 24 h. The strength loss observed here is due to changes in the local environment at the glass surface rather than an aging phenomenon or changes in the nature of the glass surface. This strength loss is recoverable, since the strength of bare fiber (5.1 GPa under equivalent conditions) does not change with preconditioning over a 24-h period. If the coating were merely acting as a diffusion barrier, then the equilibrium strength of coated fiber would be the same as the strength of bare fiber. However, the coating can change the local environment at the glass surface, for example by perhaps passivating it[17] or by changing the local pH,[18] or, using suitable additives, by slowing strength-degrading chemical reactions.[19]

These results show that if coated fiber is not correctly preconditioned with the test environment the apparent values of $n$ will be too low. This effect might explain the uncharacteristically low values of $n$ observed by Yuce *et al.*[2] Additionally, poor equilibration might produce an apparent loading mode effect if the experiments for the different modes span different test times. The slowest loading rates in Table I, for example, give a test time of 3 h at constant faceplate velocity, but 15 h at constant stress rate.

It is noted that the strength reduction with time observed in Fig. 7 is insufficient to explain the large difference in strength observed at 60 MPa·s$^{-1}$ in Fig. 6. This implies that additional effects occur. One may speculate that stress enhances the rate of

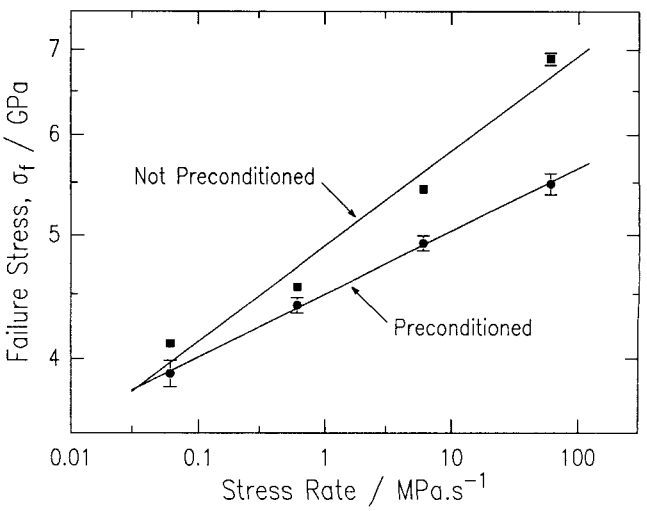


**Fig. 6.** Dynamic fatigue data under conditions of constant stress rate for fiber that has been preconditioned for 24 h in the test environment and for nonpreconditioned fiber.

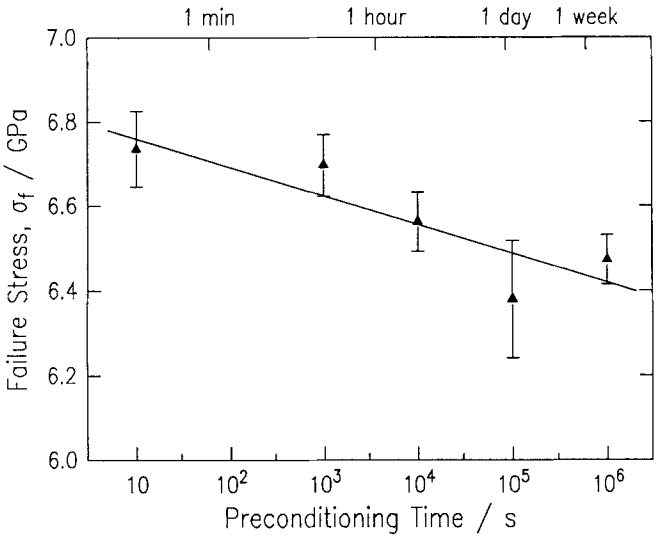


**Fig. 7.** Effect on strength of different times of preconditioning in the test environment. Strengths are measured at a constant faceplate velocity of 1000 $\mu m \cdot s^{-1}$.

effects occur. One may speculate that stress enhances the rate of equilibration, since it is well-known that diffusion coefficients for liquids through polymers increase rapidly with tensile strain.

It is clear that coated fiber should be properly equilibrated with the environment in order to obtain reliable estimates on $n$. Such equilibration should be established rather than simply assumed.

## V. Conclusions

Dynamic fatigue experiments performed in two-point bending on bare and coated silica optical fiber at constant velocity, constant stress rate, and constant strain rate show no significant differences between the values of the stress corrosion susceptibility parameter, $n$, and the crack growth preexponent, $A$, calculated for the three loading modes. This indicates that two-point bending does provide reliable results for fatigue properties, at constant faceplate velocity in particular. However, for direct numerical comparison of bending and tension strengths, the bending experiment should be conducted at constant stress or strain rate. It is shown that these results are not dependent on the form of the crack growth kinetics model.

Significant differences between the values of $n$ are evident when they are calculated from the slope of log (failure strain) versus log (loading rate) plots instead of the usual log (failure stress) versus log (loading rate) plots. This difference, which is due to the strain dependence of the elastic modulus of silica, is significant only for high-strength material.

It is shown that if the fiber is stored in one environment and tested in another and insufficient time is allowed for preconditioning in the test environment, significant perturbation on the value of $n$ for coated fiber can result. The apparent value of $n$ is reduced if the storage environment is less aggressive than the test environment; it is increased if the storage environment is more aggressive. It is therefore necessary to establish that the fiber is equilibrated with the test environment before relying on the value of $n$ determined for coated fiber.

## References

[1]M. J. Matthewson, C. R. Kurkjian, and S. T. Gulati, "Strength Measurement of Optical Fibers by Bending," *J. Am. Ceram. Soc.*, **69** [11] 815–21 (1986).

[2]H. H. Yuce, M. E. Melczer, and P. L. Key, "Mechanical Properties of Optical Fibers in Bending"; pp. 44–55 in IOOC '89 Technical Digest (proceedings of the 7th International Conference on Integrated Optics and Optical Fiber Communications, July 18–21, 1989). Optical Society of America, Washington, DC, 1989.

[3]C. R. Kurkjian, J. T. Krause, and U. C. Paek, "Tensile Strength Characteristics of "Perfect" Silica Fibers," *J. Phys.*, **43** [12] C9-585, 586 (1982).

[4]P. W. France, M. J. Paradine, M. H. Reeve, and G. R. Newns, "Liquid Nitrogen Strengths of Coated Optical Glass Fibres," *J. Mater. Sci.*, **15**, 825–30 (1980).

[5]S. M. Wiederhorn, "Subcritical Crack Growth in Ceramics"; pp. 613–46 in *Fracture Mechanics of Ceramics*, Vol. 2. Edited by R. C. Bradt, D. P. H. Hasselman, and F. F. Lange. Plenum Press, New York, 1974.

[6]P. W. France, M. J. Paradine, and K. J. Beales, "Ultimate Strengths of Glasses Used for Optical Communications"; in Proceedings of the 12th International Congress on Glass, Albuquerque, NM. North-Holland, Amsterdam, Netherlands, 1980.

[7]J. T. Krause, L. R. Testardi, and R. N. Thurston, "Deviations from Linearity in the Dependence of Elongation upon Force for Fibres of Simple Glass Formers and of Glass Optical Lightguides," *Phys. Chem. Glasses*, **20** [6] 135–39 (1979).

[8]G. S. Glaesemann, S. T. Gulati, and J. D. Helfinstine, "Effect of Strain and Surface Composition on Young's Modulus of Optical Fibers"; in *Technical Digest, Optical Fiber Communications Conference*, Paper TUG5. Optical Society of America, Washington, DC, 1988.

[9]G. S. Glaesemann and S. T. Gulati, "Dynamic Fatigue Data for Fatigue Resistant Fiber in Tension vs Bending"; in *Technical Digest, Optical Fiber Communications Conference*, Paper WA3. Optical Society of America, Washington, DC, 1989.

[10]J. T. Krause and C. J. Shute, "Temperature Dependence of the Transition in Static Fatigue of Fused Silica Optical Fiber," *Adv. Ceram. Mater.*, **3** [2] 118–21 (1988).

[11]V. V. Rondinella, M. J. Matthewson, and B. Lin, "Influence of Solutes on the Fatigue Behavior of Pristine Silica Optical Fiber," *Ceram. Trans.*, **20**, 171–82 (1991).

[12]M. J. Matthewson, V. V. Rondinella, B. Lin, and S. W. Keyes, "Effect of Alkali Hydroxides on the Strength and Fatigue of Fused Silica Optical Fiber," *J. Am. Ceram. Soc.*, **74** [10] 2592–98 (1991).

[13]G. G. Trantina, "Strength and Life Prediction for Hot-Pressed Silicon Nitride," *J. Am. Ceram. Soc.*, **62** [7–8] 377–80 (1979).

[14]K. Jakus, J. E. Ritter, and J. M. Sullivan, "Dependency of Fatigue Predictions on the Form of the Crack Velocity Equation," *J. Am. Ceram. Soc.*, **64** [6] 372–74 (1981).

[15]G. M. Bubel and M. J. Matthewson, "Optical Fiber Reliability Implications of Uncertainty in the Fatigue Crack Growth Model," *Opt. Eng.*, **30** [6] 737–45 (1991).

[16]M. J. Matthewson, "Fiber Lifetime Predictions," *Proc. SPIE—Int. Soc. Opt. Eng.*, **1580** (Fiber Optics Reliability: Benign and Adverse Environments V), 130–41 (1992).

[17]J. P. Clarkin, B. J. Skutnik, and B. D. Munsey, "Enhanced Strength and Fatigue Resistance of Silica Fibers with Hard Polymeric Coatings," *J. Non-Cryst. Solids*, **102**, 106–11 (1988).

[18]M. J. Matthewson and C. R. Kurkjian, "Environmental Effects on the Static Fatigue of Silica Optical Fiber," *J. Am. Ceram. Soc.*, **71** [3] 177–83 (1988).

[19]V. V. Rondinella, M. J. Matthewson, and C. R. Kurkjian, "Coating Additives for Improved Mechanical Reliability of Optical Fiber," *J. Am. Ceram. Soc.*, in review. □